

# Ground- and Excited-State Spectroscopic Studies on [1-(4-Methoxyphenyl)-3-(amino)-2,4-(dicyano)-9,10-tetrahydrophenanthrene]

Ibrahim A. Z. Al-Ansari<sup>1</sup>

Received November 18, 1994; accepted August 2, 1995

The effects of polar and nonpolar solvents on both the ground and the excited-state properties of [1-(4-methoxyphenyl)-3-(amino)-2,4-(dicyano)-9,10-tetrahydrophenanthrene] is examined. Light absorption results in a population of a locally excited (LE) first singlet state ( $S_1, n\pi^*$ ) which shows sensitivity to the polarity of the surrounding solvent and hydrogen-bonding ability to the quencher 4-methylpyridine. Relaxation of this state leads to an intramolecular charge-transfer state (ICT) which leads to a large Stokes shift in polar solvents and an excited-state dipole moment of  $\mu_e = 10D$ . The quenching of the fluorescence state by 4-methylpyridine studied in *n*-hexane and acetonitrile at room temperature is found to be efficient and a positive deviation from linearity was observed in the Stern–Volmer plots even at concentrations of 4-methylpyridine below 0.4 *M*. This is explained as a result of the occurrence of both a dynamic and a static quenching mechanism. The static quenching constants ( $K_{sv}$ ) along with those obtained by visible spectroscopy ( $K_{GS}$ ) indicate that the ground-state complex is weak and relatively solvent dependent.

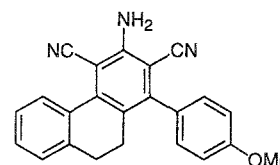
**KEY WORDS:** Absorption; fluorescence; solvent effect; charge transfer; dipole moment; quenching; ground-state complexation.

## INTRODUCTION

For many years intensive work has been carried out on the ground-state complexes of charge transfer characters between aromatic hydrocarbons and chlorinated alkanes.<sup>(1–5)</sup> On the other hand, studies show that intermolecular hydrogen bonding in many molecules usually leads to modification of their photophysical properties including fluorescence quenching through hydrogen bonding interaction.<sup>(6–17)</sup>

In this work, we have examined the absorption, fluorescence, and ground-state charge-transfer complexation between 4-methylpyridine (4-MP) and the new compound [1-(4-methoxyphenyl)-3-(amino)-2,4-(dicyano)-9,10-tetrahydrophenanthrene] (MPACTP). Also,

the effect of solvent polarity on the fluorescence quenching mechanism of the system MPACTP/4-MP was investigated. We present evidence for the formation of 1:1 intermolecular complexes between MPACTP and 4-MP in the ground state in *n*-hexane and acetonitrile solvents, which involve the participation of the –NH group of the compound MPACTP. Fluorescence data also suggest that 4-MP acts as an efficient quencher up to a concentration of 0.8 *M*.



MPACTP

<sup>1</sup> Department of Chemistry, Faculty of Science, University of Qatar, P.O. Box 2713, Doha, Qatar.

## EXPERIMENTAL

### Materials

$\alpha$ -Tetalone, cyanoacetamide, piperidine, and malonitrile were purchased from Fluka Chemical Co. The titled compound, MPACTP, was synthesized by a procedure similar to that for pyridine-2(1*H*)-thiones.<sup>(18)</sup> The organic solvents used (*n*-hexane, chloroform, dichloromethane, carbon tetrachloride, ethanol, methanol, butanol, diethyl ether, dimethylformamide, and acetonitrile) were all of spectrophotometric grade (BDH Chemical Co.)

*Synthesis of Phenylcyanoheptyl Malonitrile (1): 95% yield.*  $\alpha$ -Tetalone (0.1 *M*, 14.6 g) was mixed with malonitrile (0.1 *M*, 6.6 g) in 30 cm<sup>3</sup> ethanol and an excess amount of triethylamine (0.15 *M*, 6 cm<sup>3</sup>). The mixture was stirred and refluxed for 2 h; after cooling the product was collected and recrystallized from ethanol to give a white-yellowish powder; m.p = 103–104°C, <sup>1</sup>H NMR (400 MHz, DMSO-*d*<sub>6</sub>)  $\delta$  1.8–2.0 (d,d, 2H)  $\delta$  2.7–3.0 (m, 2H)  $\delta$  3.3 (s, 2H)  $\delta$  7.4–8.3 (m, Ar-H). IR (KBr)  $\bar{\nu}$  152 cm<sup>-1</sup> (C=C),  $\bar{\nu}$  1566.1 cm<sup>-1</sup> (C=N),  $\bar{\nu}$  2964 cm<sup>-1</sup> (C-H).

*Synthesis of 4-Methoxyphenyl Methylenecyanoacetamide (2): 90% yield.* *p*-Methoxybenzaldehyde (0.1 *M*, 13.6 g) and cyanoacetamide (0.1 *M*, 0.84 g) were mixed in 30 cm<sup>3</sup> ethanol and the mixture was stirred and refluxed for 2 h in piperidine (0.15 *M*, 6 cm<sup>3</sup>). The product separated on cooling and was collected, washed with cold ethanol, and then recrystallized to yield pure product as white powder; m.p = 189–199°C. <sup>1</sup>H NMR (400 MHz, DMSO-*d*<sub>6</sub>)  $\delta$  3.34 (s, -NH<sub>2</sub>)  $\delta$  3.86 (s, -OCH<sub>3</sub>)  $\delta$  7.08–8.12 (m, Ar-H). IR (KBr)  $\bar{\nu}$  1509.7 cm<sup>-1</sup> (C=C),  $\bar{\nu}$  2210.3 cm<sup>-1</sup> (C=N),  $\bar{\nu}$  3299.1 cm<sup>-1</sup> and  $\bar{\nu}$  3359.0 cm<sup>-1</sup> (typical amide -NH<sub>2</sub> pair of bands).

*Synthesis of [1-(4-Methoxyphenyl)-3-(amino)-2,4-(dicyano)-9,10-tetrahydrophenanthrene] (MPACTP): 45% yield.* A few drops of piperidine was added to a mixture of compound **1** (0.008 *M*, 1.55 g) and compound **2** (0.008 *M*, 1.61 g) dissolved in absolute ethanol (25 cm<sup>3</sup>). The mixture was stirred and refluxed for 6 h. After cooling the precipitated solid product MPACTP was collected and recrystallized from ethanol to give white-yellowish crystals; m.p = 168–169°C. The structure of compound MPACTP was confirmed by <sup>1</sup>H NMR and GC/MS. The mass spectrum was compatible with the molecular formula C<sub>23</sub>H<sub>17</sub>N<sub>3</sub>O (M<sup>+</sup>, 351) and <sup>1</sup>H NMR (400 MHz, DMSO-*d*<sub>6</sub>)  $\delta$  3.85 (s, -OCH<sub>3</sub>),  $\delta$  7.15–7.55 (m, Ar-H) 6.4 (br, -NH<sub>2</sub>).

### Sample Preparation

Stock solutions (10<sup>-4</sup> M) of the compound MPACTP was prepared by dissolving the accurate amount of it in

cyclohexane, from which 1 ml was withdrawn and added to a 10-ml flask. This was then evaporated by nitrogen bubbling to leave a thin film. The desired solvent was added and completed to the mark to give a 10<sup>-5</sup> M solution.

### Spectroscopic Measurements

Electronic absorption spectra of the compound were recorded on a Shimadzu UV-160 spectrometer at 22°C using 1-cm matched quartz cells. Emission spectra were obtained on a Shimadzu RF-500 spectrometer using small-angle (22.5°) front surface excitation geometry. Excitation and emission slits were both 0.5 nm. Excitation wavelength ( $\lambda_{exc}$ ) = 350 nm. Fresh solutions were used for all measurements. Fluorescence spectra were corrected for wavelength-dependent instrument response. The experiments were carried out at room temperature (23°C).

### Quantum Yield Measurements

The emission quantum yield of a sample X { $\phi_f(X)$ } was calculated using a solution of quinine sulfate in 0.1 *N* sulfuric acid as a reference, that has a quantum yield of  $\phi_f(R) = 0.55$ , and applying the following formula:<sup>(19)</sup>

$$\phi_f(X) = \phi_f(R) \{n^2(X) F_R A_R I_X\} / \{n^2(R) F_X A_X I_R\} \quad (1)$$

where *n* is the refractive index of the solution, *F* is the radiant flux, *A* is the absorbance of the sample at the wavelength of excitation, and *I* is the integrated emission intensity, measured by a cut-and-weigh technique.

## RESULTS AND DISCUSSION

### Solvent Dependence of Absorption and Emission Spectra

Absorption spectra of compound MPACTP in non-polar and polar solvents consist of three separated regions of separated electronic states. The first band, mainly a  $\pi\pi^*$  state, appears at 225 nm, and the second band, with a  $\pi\pi^*$  character, appears at 270 nm. The third band was located around 360 nm. The first band is slightly sensitive to solvent polarity, however, the lowest excited S<sub>1</sub> state (the third band) is an  $n\pi^*$  and has a strong charge-transfer character in polar solvents, which leads to a strong red shift of the absorption band maxima [see Fig. 1 for absorption spectra in *n*-hexane and acetonitrile, where  $\lambda_{max}$  (*n*-hexane) = 362.2 nm (27,586 cm<sup>-1</sup>), compared to  $\lambda_{max}$  (acetonitrile) = 365.5 nm (27,360 cm<sup>-1</sup>), for a difference

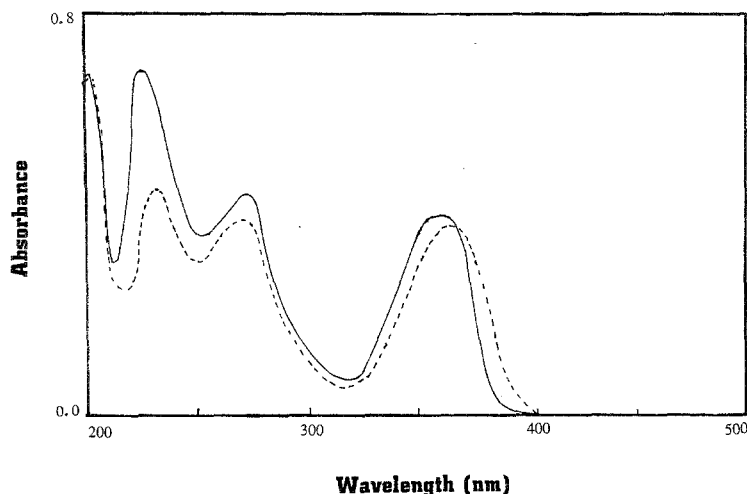


Fig. 1. Absorption spectra of compound MPACTP at room temperature in *n*-hexane (---) and acetonitrile (—). MPACTP concentration, was  $2.25 \times 10^{-5} M$ .

Table I. Absorption and Fluorescence Maxima, Stokes Shift, and Fluorescence Quantum Yields of MPACTP in Various Solvents

Solvent	$\bar{\nu}_a$ (max) ( $\text{cm}^{-1}$ )	$\bar{\nu}_f$ (max) ( $\text{cm}^{-1}$ )	$\bar{\nu}_a - \bar{\nu}_f$ ( $\text{cm}^{-1}$ )	$\phi_f$
<i>n</i> -Hexane	27,586	25,252	2334	0.291
Diethyl ether	27,211	24,272	2939	0.351
$\text{CHCl}_3$	27,357	24,390	2969	0.253
$\text{CH}_2\text{Cl}_2$	27,510	24,691	2819	0.292
DMF <sup>a</sup>	26,667	23,474	3193	0.290
$\text{CH}_3\text{CN}$	27,360	24,038	3322	0.206

<sup>a</sup> Dimethylformamide.

of  $226.4 \text{ cm}^{-1}$ ]. Table I compiles absorption data of MPACTP in different solvents.

In alcohols, the charge-transfer (CT) band is more pronounced and appears at lower energy than in other polar non-hydrogen bonding solvents. The reason for this phenomenon appears to be due to enhancement of the CT state in alcohols as a result of hydrogen bonding complexation compared to polar aprotic solvents. For instance, the absorption maximum of MPACTP in acetonitrile ( $\epsilon = 37.5$ ) is at  $365.5 \text{ nm}$ , and in ethanol ( $\epsilon = 24.30$ ) it is located at  $368.5 \text{ nm}$ . Furthermore, the CT band red-shifts in highly acidic media with intensity enhancement (see Fig. 2). This band also appears as two distinct peaks with a shoulder around  $320 \text{ nm}$ . It appears that in acidified alcohols, protonation occurs on the  $-\text{NH}$  group, thus enhancing the electron withdrawing capability and hence facilitating CT transition. The second

band in highly acidic alcoholic solution such as in  $\text{H}_2\text{SO}_4$  blue-shifts with a fine vibrational character.

Figure 3 shows the normalized absorption and fluorescence spectra of compound MPACTP in *n*-hexane. The fluorescence maxima in *n*-hexane appears at  $398 \text{ nm}$  ( $23125 \text{ cm}^{-1}$ ), with a long-wavelength tail extending to  $500 \text{ nm}$ . Table I lists the fluorescence maximum wavelength in different solvents, along with the spectral shift between the CT absorption and the fluorescence maxima. It is obvious that the difference between the locally excited state (LE) and the charge-transfer state (CT) is solvent dependent, from which the excited-state dipole moment can be obtained. Quantum yields of the fluorescence state are in the same range and solvent polarity independent (see Table I).

### Hydrogen-Bonding Effects on Absorption Spectra

The ground-state equilibrium constants ( $K_{\text{GS}}$ ) of 1:1 hydrogen bonding for the MPACTP/4-MP pair in *n*-hexane and acetonitrile at room temperature were obtained from analysis of the concentration effect of 4-MP on the MPACTP absorption spectrum.

The ground-state absorption spectrum of MPACTP is changed upon addition of 4-MP to its *n*-hexane and acetonitrile solutions. A general increase in the intensity of the absorbance of MPACTP is observed with increasing 4-MP concentration. The  $n\pi^*$  ( $S_0 \rightarrow S_1$ ) charge-transfer band is slightly red-shifted, indicating large stabilization of the excited-state. On the other hand, the second band, a  $\pi\pi^*$  ( $S_0 \rightarrow S_2$ ) with considerable charge

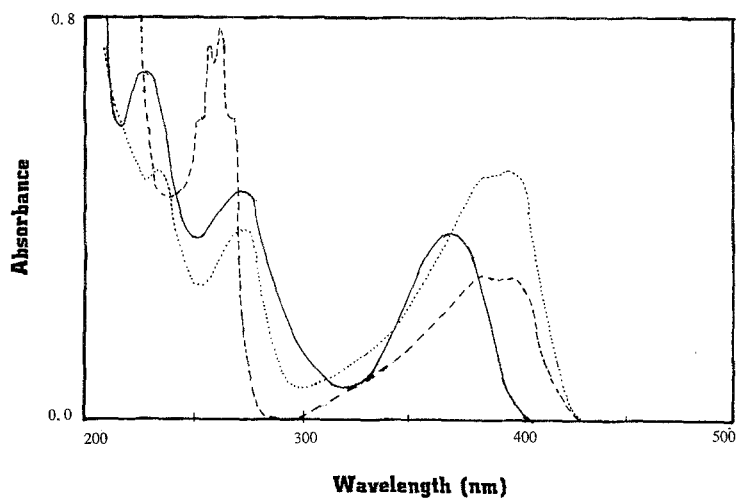


Fig. 2. Absorption spectra of compound MPACTP at room temperature in ethanol (---), ethanol + HCl (.....), and ethanol + H<sub>2</sub>SO<sub>4</sub> (—).

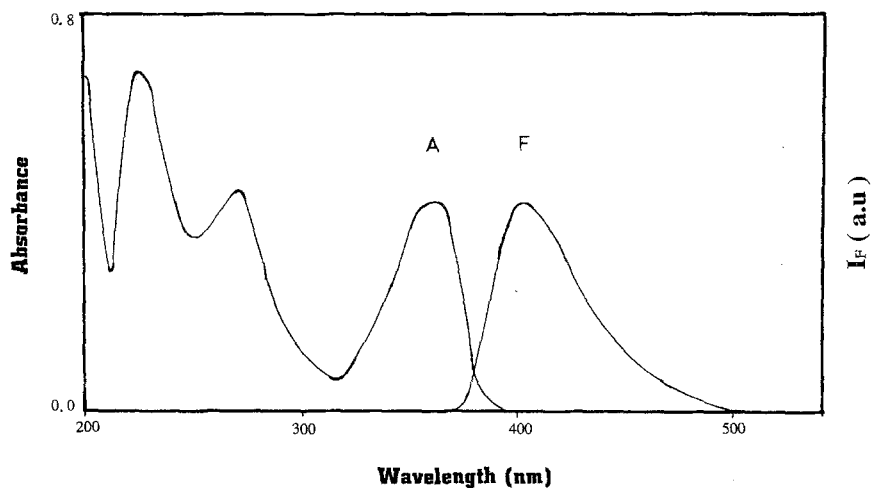


Fig. 3. Normalized absorption and fluorescence ( $\lambda_{exc} = 350$  nm) spectra of compound MPACTP at room temperature in *n*-hexane.

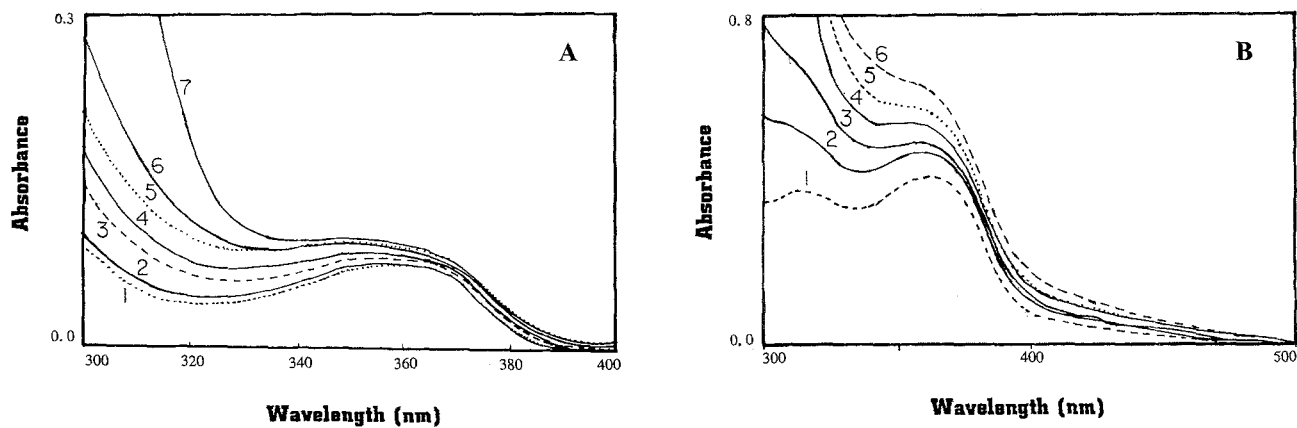


Fig. 4. The changes in the visible absorption spectra of MPACTP: (A) in *n*-hexane at 4-MP concentrations of (1) 0 *M*, (2)  $1 \times 10^{-5}$  *M*, (3)  $5 \times 10^{-5}$  *M*, (4)  $8 \times 10^{-5}$  *M*, (5)  $5 \times 10^{-2}$  *M*, (6) 0.1 *M*, and (7) 0.2 *M*; (B) in acetonitrile at 4-MP concentrations of (1) 0 *M*, (2)  $1 \times 10^{-5}$  *M*, (3)  $5 \times 10^{-5}$  *M*, (4)  $8 \times 10^{-5}$  *M*, (5)  $5 \times 10^{-2}$  *M*, and (6) 0.1 *M*.

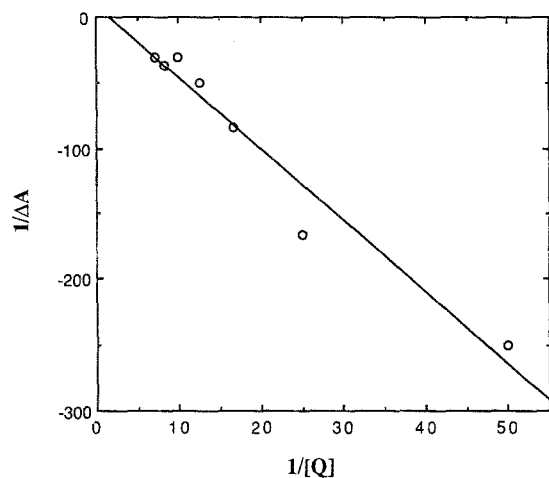


Fig. 5. Benesi-Hildebrand plots [according to Eq. (2)] for MPACTP in *n*-hexane as a function of 4-MP concentration. The straight lines are linear regression fits to the experimental data points.

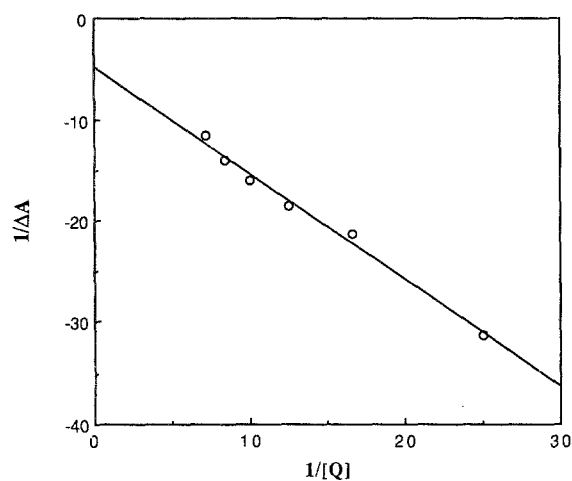


Fig. 6. Benesi-Hildebrand plots [according to Eq. (2)] for MPACTP in acetonitrile as a function of 4-MP concentration. The straight lines are linear regression fits to the experimental data points.

Table II. Ground-State Association Constant ( $K_{GS}$ ) Values and Stern-Volmer Quenching Constant ( $K_{SV}$ ) Values for the MPACTP/4-MP System in *n*-Hexane and Acetonitrile at 300 K

Solvent	Dielectric constant ( $\epsilon$ )	$K_{GS}$ ( $M^{-1}$ ) from Benesi-Hildebrand plots	$K_{SV}$ ( $M^{-1}$ ) from linear range in Fig. 10
<i>n</i> -Hexane	1.890	2.0	4.20
Acetonitrile	37.50	5.0	6.30

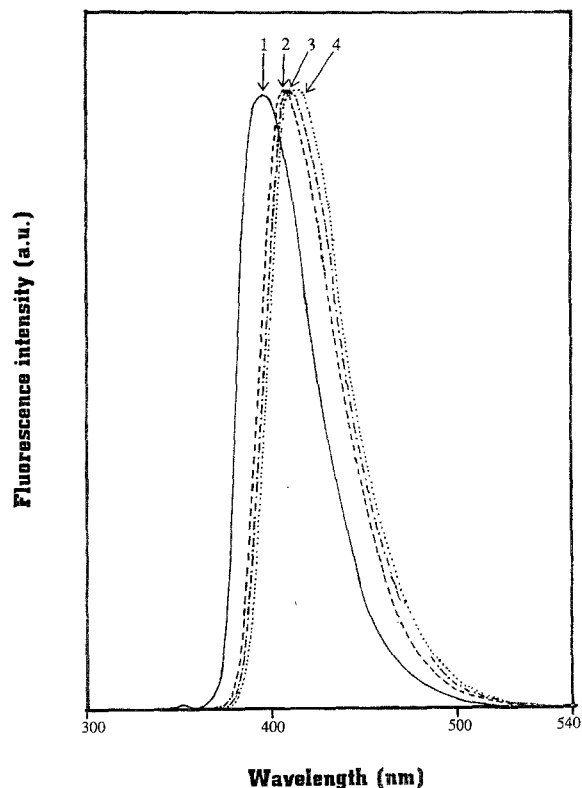


Fig. 7. Fluorescence spectra of compound MPACTP at room temperature in different solvents: 1 (—) *n*-hexane, 2 (—)  $CHCl_3$ , 3 (---) diethyl ether, and 4 (.....) acetonitrile.

transfer, is blue-shifted, owing to increasing the transition energy gap to this state.

Figures 4A and B give the long-wavelength absorption band of MPACTP in *n*-hexane and acetonitrile, respectively, which clearly show that the addition of 4-MP increases the intensity of the long-wavelength band with a shift of the tail to lower energy. Further, it can be seen from Figs. 4A and B that the relative increase in absorbance when 4-MP is added is largest in the shorter-wavelength region.

We attempted to use the Benesi-Hildebrand equation to interpret the spectral shift in the absorption based on 1:1 hydrogen bonding:<sup>(20)</sup>

$$1/\Delta A = 1/\Delta \epsilon [\text{MPACTP}] + 1/\Delta \epsilon [\text{MPACTP}] K_{GS} [4\text{-MP}] \quad (2)$$

where  $\Delta \epsilon = \epsilon_f - \epsilon_a$  ( $\epsilon_f$  and  $\epsilon_a$  are the molar absorptivities of the free MPACTP and the complexed MPACTP molecules, respectively).

The results of Eq. (2) are shown in Figs. 5 and 6 (based on absorbance at  $\lambda = 360$  nm) for *n*-hexane and acetonitrile solutions. From these plots the ground-state

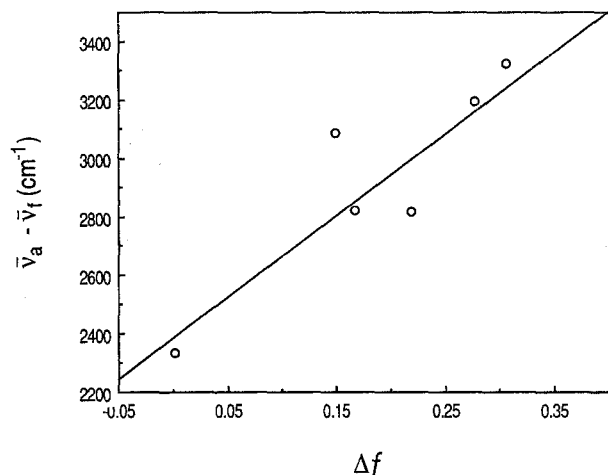


Fig. 8. Dependence of  $\bar{\nu}_a - \bar{\nu}_f$  of MPACTP on the solvent polarity parameter  $\Delta f = f - f'$ .

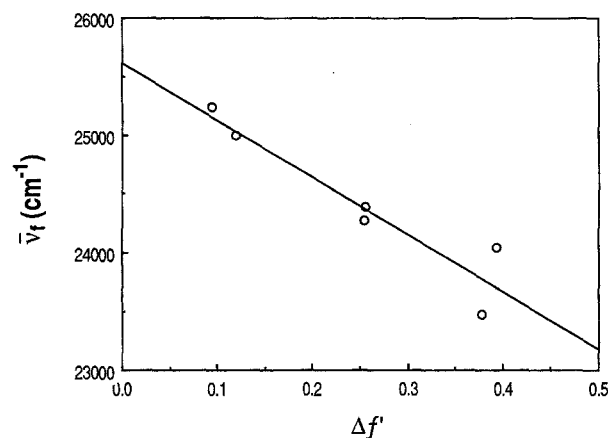


Fig. 9. Dependence of  $\bar{\nu}_f$  of MPACTP on the solvent polarity parameter  $\Delta f' = f - f'/2$ .

Table III. Values of the Ground- and Excited-State Dipole Moments [in Debye Units (D)] According to Eqs. (6) and (7), for Compound MPACTP

$a$ (Å) <sup>a</sup>	Slope <sup>b</sup>		$\mu_g$ (D) <sup>c</sup>	$\mu_e$ (D) <sup>d</sup>
	$\Delta f$	$\Delta f'$		
5.52	2920.0	4875.6	2.30	10.0

<sup>a</sup> Onsager cavity radius.

<sup>b</sup> Obtained from Eqs. (6) and (7).

<sup>c</sup> Calculated according to Eq. (6).

<sup>d</sup> Calculated according to Eq. (7).

equilibrium constants (see Table II) are obtained, where  $K_{GS} = [D-H \cdots A]/[D-H][A]$  for the equilibrium:

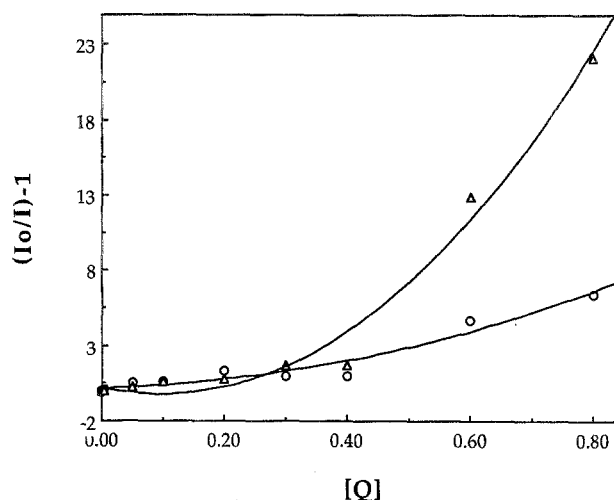
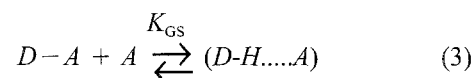


Fig. 10. Stern-Volmer plot of  $(I_0/I) - 1$  against 4-MP concentration in (○) *n*-hexane and (△) acetonitrile.



The values of  $K_{GS}$  obtained (see Table II) indicate a weak ground-state charge transfer for complex MPACTP/4-MP in *n*-hexane and a relatively higher value in acetonitrile, which is indicative of a more stabilized complex in the latter solvent.

The plots of Eq. (2) give a good linear relationship, with correlation coefficients of 0.952 and 0.990 for *n*-hexane and acetonitrile solutions, respectively. These results indicate the validity of the 1:1 hydrogen complexation.

### Ground- and Excited-State Dipole Moments

The fluorescence energy maxima is sensitive to solvent polarity (see Fig. 7 and Table I). The bathochromic shift observed for the fluorescence is  $1214 \text{ cm}^{-1}$  in going from *n*-hexane to acetonitrile solvent, suggesting that the state responsible for this emission is of a highly charge-transfer (CT) nature. This is also supported by the structureless shape of the fluorescence bands.

Figure 8 shows the dependence of the Stokes' shift,  $\bar{\nu}_a - \bar{\nu}_f$ , on the solvent polarity parameter  $\Delta f = f - f'$ ,<sup>(21)</sup> where

$$f = (\epsilon - 1)/(2\epsilon + 1) \quad (4)$$

$$f' = (n^2 - 1)/(2n^2 + 1) \quad (5)$$

and  $\epsilon$  and  $n$  are the solvent static dielectric constants and refractive index, respectively. Figure 9 shows that a lin-

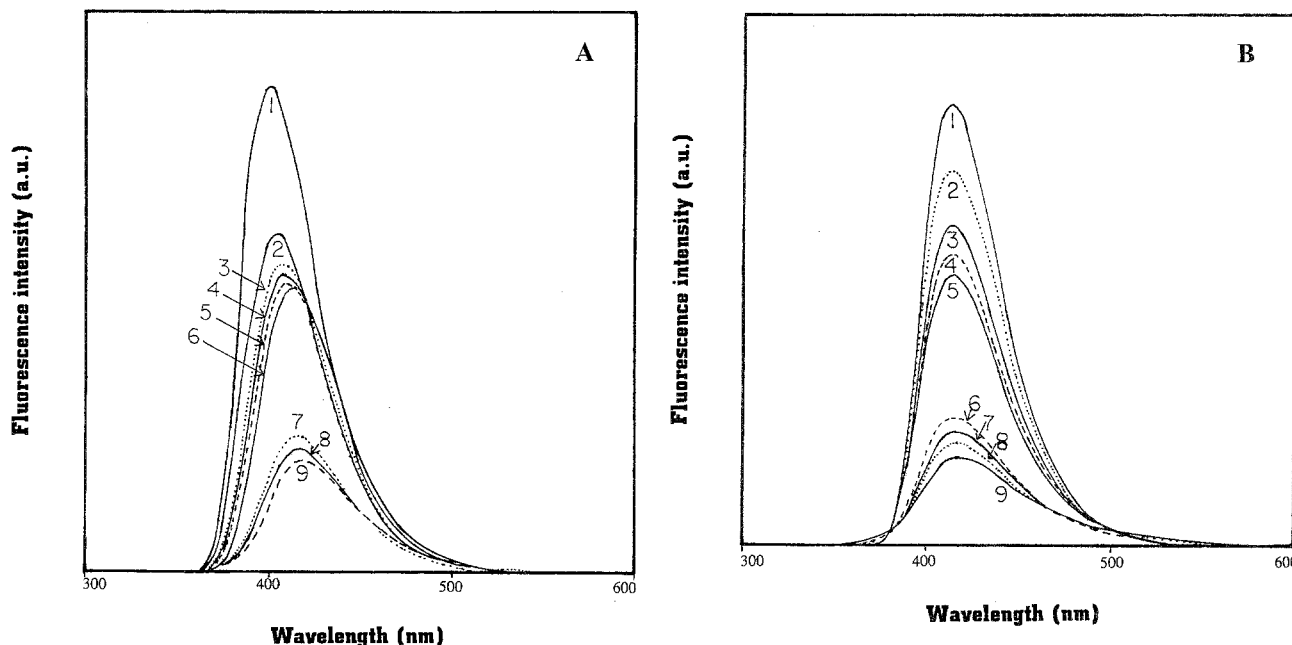


Fig. 11. Fluorescence spectra of MPACTP at  $\lambda_{\text{exc}} = 350 \text{ nm}$ : (A) in *n*-hexane at 4-MP concentrations of (1) 0 *M*, (2) 0.02 *M*, (3) 0.06 *M*, (4) 0.08 *M*, (5) 0.12 *M*, (6) 0.14 *M*, (7) 0.18 *M*, (8) 0.24 *M*, (9) 0.3 *M*, and (10) 0.4 *M*; (B) in acetonitrile at 4-MP concentrations of (1) 0 *M*, (2) 0.02 *M*, (3) 0.06 *M*, (4) 0.08 *M*, (5) 0.12 *M*, (6) 0.14 *M*, (7) 0.18 *M*, (8) 0.24 *M*, (9) 0.3 *M*; and (10) 0.4 *M*.

ear relation between the fluorescence band maxima ( $\bar{\nu}_f$ ) and the solvent polarity parameter  $\Delta f' = f - f/2^{(21)}$  exists. The results of the regression analysis reported in Fig. 8 give a correlation coefficient of 0.82.

The excited-state dipole moment is obtained from the linear relation in Fig. 10, which depends on the following equation:<sup>(22)</sup>

$$\bar{\nu}_f = \bar{\nu}(0) - \frac{2\mu_e^2 \Delta f'}{hca^3} \quad (6)$$

where  $\bar{\nu}(0)$  is the gas-phase value for the fluorescence energy level,  $\mu_e$  is the dipole moment for the fluorescence excited-state,  $a$  is the Onsager cavity radius,<sup>(22)</sup> taken as 40% of the longitudinal axis of the compound (roughly estimated to be 5.52 Å, obtained from a molecular mechanics program,<sup>(23)</sup>) and  $h$  and  $c$  are fundamental constants.

From the slope of the fitted curve in Fig. 9, the charge-transfer (ICT) dipole moment  $\mu_e = 10.0\text{D}$  is obtained (see Table III). The linear relation in Fig. 9 (with a correlation coefficient of 0.892) corresponds to the equation<sup>(21)</sup>

$$\Delta\bar{\nu} = \frac{2\Delta\mu^2 \Delta f'}{hca^3} \quad (7)$$

where  $\Delta\bar{\nu} = \bar{\nu}_a - \bar{\nu}_f$  ( $\bar{\nu}_a$  and  $\bar{\nu}_f$  are the wavenumbers of the absorption and fluorescence maxima, respectively)

and  $\Delta\mu = \mu_e - \mu_g$  ( $\mu_g$  is the ground-state dipole moment). Based on the slope in Fig. 9, a value of  $\mu_g = 2.3 \text{ D}$  is obtained.

### Excited-State Quenching Mechanism

To see whether excited-state complex formation involving a 1:1 intermolecular hydrogen bonding exists following excitation of the MPACTP/4-MP system, we studied the quenching processes in the excited state. The Stern–Volmer equation,<sup>(24)</sup>

$$\frac{I_0}{I} = 1 + K_{\text{sv}} [Q] \quad (8)$$

is used for this purpose, where  $K_{\text{sv}}$  is the Stern–Volmer quenching constant. At low concentrations of 4-MP linear curves were obtained to 0.2 *M* in both solvents, but at higher concentrations the curves show a positive deviation from linearity.

Figure 10 shows plots of Eq. (8) in *n*-hexane and acetonitrile. These nonlinear plots indicate that quenching occurs via a dynamic and a static mechanism, which was confirmed above. The linear dependence of  $I_0/I$  versus  $[Q]$  at lower quenching concentrations indicates the presence of a dynamic quenching mode, while the positive deviation from linearity suggests contributions of both a dynamic and a static quenching mechanism. The

deviation from linearity in the polar solvent acetonitrile is larger compared to *n*-hexane, suggesting stronger ground-state complexation (see Table II for the values of  $K_{SV}$  in these solvents). The values of the quenching constants obtained by fluorescence quenching studies are slightly higher than those obtained by absorption studies. These differences may be due to stabilization of the complex through charge transfer from MPACTP to the 4-MP quencher in the excited state. Thus quenching is relatively higher in the excited state than the ground state. Such a mechanism is also given for the quenching of the pyridylinoles<sup>(25)</sup> and aminopyrene<sup>(26)</sup> by hydrogen-bond acceptors, such as alcohols and pyridine, respectively. Compounds such as MPACTP, which possess hydrogen-bond groups like-NH, also tend to transfer electrons to the hydrogen-bond acceptor pyridine in the excited state.

Figures 11A and B show the fluorescence spectral changes on adding the quencher 4-MP. Beside the obvious quenching efficiency of the quencher, it is seen that fluorescence maxima shift to a longer wavelength (from  $\lambda_{max} = 400$  nm in the absence of the quencher to  $\lambda_{max} = 418$  nm in 0.4 M quencher in *n*-hexane and from  $\lambda_{max} = 412$  nm in the absence of the quencher to  $\lambda_{max} = 420$  nm in 0.4 M quencher in acetonitrile). Such behavior confirms that intermolecular hydrogen bonding indeed facilitates a charge transfer to the pyridine moiety.

## REFERENCES

1. R. Anderson and J. M. Prausnitz (1963) *J. Chem. Phys.* **39**, 1225.
2. R. F. Weimer and J. M. Prausnitz (1965) *J. Chem. Phys.* **42**, 3643.
3. N. C. Perrins and J. P. Simons (1969) *Trans. Faraday Soc.* **65**, 390.
4. H. O. Hooper (1964) *J. Chem. Phys.* **41**, 599.
5. W. G. Rothschild (1971) *Chem. Phys. Lett.* **9**, 149.
6. N. Mataga and S. Tsuni (1956) *Naturwissenschaften* **10**, 305.
7. D. Rem and A. Weller (1970) *Isr. J. Chem.* **8**, 259.
8. K. Kikuchi, H. Watari, and M. Koizumi (1973) *Bull. Chem. Soc. Jpn.* **46**, 749. S. Yamamoto, K. Kikuchi, and H. Kokubun (1976) *Bull. Chem. Soc. Jpn.* **49**, 2950.
9. M. M. Martin and W. R. Ware (1978) *J. Phys. Chem.* **82**, 2770.
10. M. M. Martin, N. Ikeda, T. Okado, and N. Mataga. (1982) *J. Phys. Chem.* **86**, 4148.
11. N. Ikeda, T. Okada, and N. Mataga (1980) *Chem. Phys. Lett.* **69**, 251. N. Ikeda, T. Okada, and N. Mataga (1981) *Bull. Chem. Soc. Jpn.* **54**, 1025.
12. N. Ikeda, H. Miyasaka, T. Okada, and N. Mataga (1983) *J. Am. Chem. Soc.* **105**, 5206.
13. M. M. Martin, H. Miyasaka, A. Karen, and N. Mataga (1985) *J. Phys. Chem.* **89**, 182.
14. J. Waluk, S. J. Komorowski, and J. Herbich (1986) *J. Phys. Chem.* **90**, 3868.
15. J. Waluk and S. J. Komorowski (1987) *Chem. Phys. Lett.* **133**, 368; (1986) *J. Mol. Struct.* **142**, 159.
16. J. Herbich, W. Rettig, R. P. Thummel, and J. Waluk (1992) *Chem. Phys. Lett.* **195**, 556.
17. H. Miyasaka, A. Tabata, K. Kamada, and N. Mataga (1993) *J. Am. Chem. Soc.* **115**, 7335.
18. G. E. H. El-gemeie, A. M. Elzanate, and A. K. Mansour (1992) *J. Chem. Soc. Perkin. Trans.* **1**, 1073.
19. J. B. Birks (1970) in *Photophysics of Aromatic Molecules*, John Wiley & Sons, NY, Chap. 4.
20. H. A. Benesi and J. H. Hildebrand (1949) *J. Am. Chem. Soc.* **71**, 2703.
21. (a) N. Mataga, Y. Kaifu, and M. Koizumi (1956) *Bull. Chem. Soc. Jpn.* **29**, 465. (b) E. Lippert (1975) in J. B. Birks (Ed.), *Organic Molecular Photophysics*, John Wiley and Sons, London, Vol. 2, p. 1. (c) E. Lippert (1957) *Z. Elektrochem.* **61**, 962. (d) L. R. Khundkar, A. E. Stiegman, and J. W. Perry (1990) *J. Phys. Chem.* **94**, 1224.
22. H. Beens, H. Knibbe, and A. Weller (1967) *J. Chem. Phys.* **47**, 1183.
23. Program MMX (89.0), a modified version of MM2 "Molecular Mechanics," was obtained from Serena Software, Bloomington, IN.
24. J. A. Baltrop and J. D. Coyle (1978) *Principles of Photochemistry*, John Wiley and Sons, New York, p. 110.
25. (a) J. Herbich, W. Rettig, R. P. Thummel, and J. Waluk (1992) *Chem. Phys. Lett.* **195** (5,6), 556 (b) J. Herbich, J. Waluk, R. P. Thummel, and C.-Y. Hung (1994) *J. Photochem. Photobiol. A Chem.* **80**, 157.
26. H. Miyasaka, A. Tabata, K. Kamada, and N. Mataga (1993) *J. Am. Chem. Soc.* **115**, 7335.